Chapter 16
Aneurysms

Barry J. Doyle and Peter R. Hoskins

16.1 Aneurysms

16.1.1 Introduction to Aneurysms

An aneurysm is a localised increase in the diameter of an artery; an outpouching of the wall. In an aneurysm there is increase in both inner and outer wall diameter, as opposed to atherosclerotic plaque where the outer wall diameter increases due to outward remodelling but the inner wall diameter (at least initially) remains unchanged.

There are 2 main types of aneurysm; the fusiform aneurysm and the saccular aneurysm (Fig. 16.1). The saccular aneurysm is often referred to as a berry aneurysm. Fusiform aneurysms most commonly occur in the abdominal aorta and to a lesser extent in popliteal arteries and in cerebral arteries. Saccular aneurysms most commonly occur in cerebral arteries, where they represent 80–90 % of all cerebral aneurysms (CAs).

Factors leading to susceptibility for aneurysm formation include both genetic and environmental factors. Hereditary conditions such as Marfan's and Ehlers-Danlos syndromes are associated with collagen disorders leading to arterial wall weakening and both these syndromes have a predisposition to aneurysms. Environmental risk factors include hypertension, cigarette smoking, family history of aneurysmal disease and oestrogen deficiency in the postmenopausal female (Mehra et al. 2011, Lasheras 2007). These risk factors translate into biological processes in the arterial wall. Development and growth of an aneurysm is an interplay between these biological processes and the mechanical environment.

B.J. Doyle (✉)
University of Western Australia, Perth, WA, Australia
e-mail: barry.doyle@uwa.edu.au

P.R. Hoskins
Edinburgh University, Edinburgh, UK
e-mail: P.Hoskins@ed.ac.uk

P.R. Hoskins et al. (eds.), *Cardiovascular Biomechanics*,
DOI 10.1007/978-3-319-46407-7_16

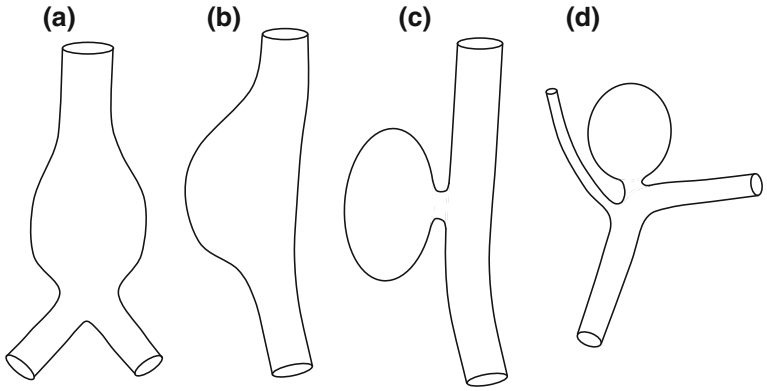

Fig. 16.1 Types of aneurysm; **a** and **b** fusiform aneurysms; **c** and **d** saccular or berry aneurysms

Development and growth of aneurysms is associated with weakening of the wall through loss of elastin with subsequent remodelling of the wall in an attempt to renormalise forces on and within the wall. The interplay between the local mechanical environment and the local biology is thought to be paramount in the initiation and growth of aneurysms, but the exact details of this relationship remain the subject of research. Once established, the aneurysm continues to grow and for some aneurysms there comes a point when the stress within the wall exceeds the wall strength and the aneurysm will rupture. Most aneurysms give no symptoms prior to rupture. The subsequent bleeding into the surrounding tissues is associated with a high mortality rate; 90 % for abdominal aortic aneurysm (AAA) rupture and 45 % for cerebral aneurysm rupture.

This chapter will concentrate on the 2 most common types of aneurysm; the abdominal aortic aneurysm and the saccular cerebral aneurysm. Further reading is provided by Lasheras (2007), Sforza et al. (2009), Humphrey and Taylor (2008), Humphrey and Holzapfel (2012), Vorp (2007), McGloughlin and Doyle (2010), Penn et al. (2011), Wong and Poon (2011) and Meng et al. (2014).

16.1.2 Aneurysms and the Law of Laplace

A simple understanding of aneurysm mechanics involves the Law of Laplace which was introduced in Chap. 5. Equations 16.1 and 16.2 describe the tension in the wall of a thin-walled cylinder and a thin-walled sphere respectively. In each case the tension T increases with diameter d.

$$T = \frac{Pd}{2} \tag{16.1}$$

$$T = \frac{Pd}{4} \tag{16.2}$$

In biomechanics it is more common to use circumferential stress H rather than tension. Equations 16.3 and 16.4 are for a thin-walled cylinder and a thin-walled sphere respectively, where w is wall thickness.

$$H = \frac{Pd}{2w} \tag{16.3}$$

$$H = \frac{Pd}{4w} \tag{16.4}$$

An artery may be considered as a thin-walled cylinder, a saccular aneurysm resembles a sphere and a fusiform aneurysm has a shape between a cylinder and a sphere. These equations suggest that the circumferential stress, and hence the risk of rupture, increases with diameter. This helps understand why diameter is the current clinical method for evaluating risk of rupture in both abdominal aortic aneurysm and in saccular CAs.

In practice there are limitations to this simple model. Arteries are not just pipes and will remodel in an attempt to normalise stresses. In practice this means that there will be changes in wall thickness as the aneurysm grows. Rupture represents mechanical failure of the tissues where circumferential stress exceeds tissue strength. The tissue strength will depend on the local tissue composition which will vary from point to point around the wall. Aneurysms have a complex geometry which does not correspond to either a cylinder or a sphere. In evaluation of rupture risk all these factors need to be accounted for, which is the aim of patient specific modelling as described in Chap. 14.

16.2 Cerebral Aneurysms

16.2.1 Cerebral Aneurysm Disease

Cerebral aneurysms are localised increases in diameter of arteries supplying the brain. These are also referred to as intracranial aneurysms. Some 4–6 % of the population aged greater than 30 years have a CA (Wardlaw and White 2000). The main clinical complication is rupture leading to bleeding. The blood accumulates beneath the arachnoid membrane which surrounds the brain, producing a subarachnoid haemorrhage. The risk of rupture of a CA is low at 0.1–1 % per year (Juvela 2004). However the consequences of rupture are severe for the patient. Mortality following aneurysm rupture is 45 %, 30 % of survivors demonstrate moderate to severe disability, and the remainder have increased risk of re-bleeds and stroke (Brisman et al. 2006). Most CAs are asymptomatic so that the first knowledge of the presence of a CA is the symptoms

associated with subarachnoid haemorrhage ('thunderclap headache', nausea, vomiting, altered consciousness of varying degree from drowsiness to complete loss of consciousness, and disturbance of vision). In some cases larger CAs may themselves produce similar symptoms immediately prior to rupture. Treatment of CAs involves a variety of procedures concerned with sealing off the aneurysm and these are considered further in Sect. 16.5.

CAs are of 2 main types, saccular and fusiform. Saccular aneurysms are round in shape and also referred to as 'berry aneurysms'; these usually occur at the branching point of arteries of the Circle of Willis and are the most common type of CA (80–90 %). Fusiform aneurysms involve an overall widening of the artery and usually do not rupture. Saccular aneurysms are also classified by size; small (<15 mm diameter), large (15–25 mm), giant (25–50 mm) and super-giant (>50 mm). The remainder of Sect. 16.2 will be concerned with saccular CAs.

16.2.2 Haemodynamics

Saccular CAs are not conduit vessels; blood flow enters and exits the aneurysm via the neck. The flow pattern within the aneurysm depends on its orientation with respect to the parent artery (Moftakher et al. 2007) (Fig. 16.2). Figure 16.2a shows a sidewall aneurysm. Flow in the aneurysm recirculates, often through the entire cardiac cycle. Blood velocity is very low, wall shear stress is very low and there is low pressure on the dome (far wall) of the aneurysm. In the case of a bifurcation

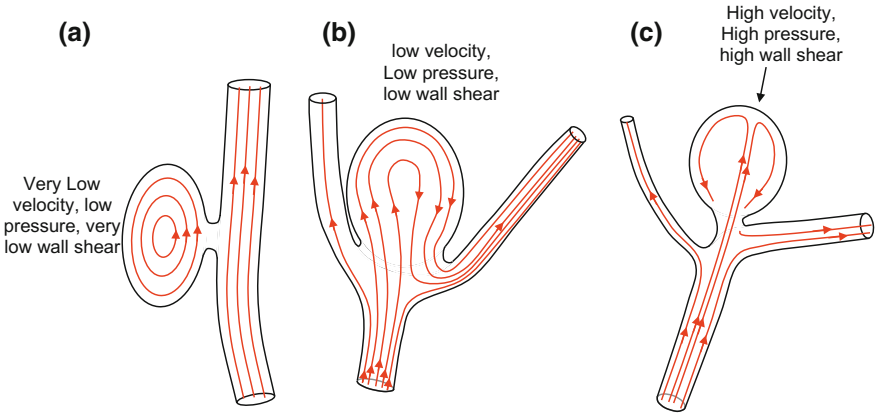

Fig. 16.2 Schematic of flow within saccular cerebral aneurysms, with indications of blood velocity, dome pressure gradient (with respect to the neck) and wall shear stress. **a** *Recirculation* recirculating flow in a side-aneurysm. **b** *Jet impact* flow from the parent artery forms a jet which impacts on the aneurysm wall. **c** *Circulating flow* flow from the parent artery enters the aneurysm through a channel in the neck, circulates as a result of the geometry of the aneurysm, and exits through a separate channel in the neck

aneurysm 2 flow patterns are seen. The most common is illustrated in Fig. 16.2b. Here flow enters the aneurysm from the parent artery through a channel within the aneurysm neck, circulates around the aneurysm, and exits through a separate channel in the neck. Velocities, wall shear and pressure at the dome are low. The second flow pattern seen in bifurcation aneurysms is illustrated in Fig. 16.2c. Here flow from the parent artery enters the aneurysm as a jet which impacts on the dome, flow then exits in a random manner through the neck. The impact of the jet causes local high wall shear and pressure on the dome. Because of the persistent flow through the cardiac cycle most CAs have no thrombus, as opposed to AAAs where thrombus is common.

16.2.3 Initiation, Growth and Rupture

The composition of cerebral arteries is different to that of systemic arteries. Cerebral arteries possess much less elastin in the medial layer, the external elastic lamina is absent, and there are structural abnormalities at the apex of bifurcations, all of which are thought to make cerebral arteries prone to saccular aneurysms. Cerebral aneurysms are characterised by loss of elastin and smooth muscle cells with consequent thinning of the medial layer (Frösen et al. 2012). Collagen fibres remodel, probably in an attempt to mechanically stabilise the aneurysm. The result is an increase in wall stiffness, with the main load-bearing performed by the adventitia rather than the media.

Initiation, growth and rupture of the CA are governed by an interplay between the mechanical environment and the local biology. The exact details of this remain the subject of research for CAs, though central to this will be presence of an intact endothelial layer. Unruptured aneurysms lack an endothelial layer (Frösen et al. 2004), and prior to this there is endothelial dysfunction. An intact endothelial layer is essential for an artery to adapt to its mechanical environment. This suggests that as the CA evolves, initially the endothelial layer is intact and the aneurysm will remodel in an attempt to normalise its mechanical environment. Later there is endothelial dysfunction with impairment in the aneurysms ability to maintain the mechanical environment. Finally there is loss of the endothelial layer and the aneurysm's ability to remodel is largely absent. Reviews of this area are provided by Sforza et al. (2009), Meng et al. (2014), Penn et al. (2011) and Selimovic et al. (2013) from which the analysis below is derived. The latter paper (Selimovic) describes computational models of aneurysm growth.

16.2.3.1 Initiation of Saccular CAs

- High wall shear stress hypothesis. Meng et al. (2014) proposed a high WSS hypothesis discussed here. At a bifurcation, flow from the parent artery impacts on the bifurcation apex producing high WSS and also a positive WSS gradient

along the flow. The endothelium detects these WSS abnormalities, and a series of biological events occurs resulting in degradation of elastin, medial thinning and formation of a bulge, which constitutes the early aneurysm.

- Low wall shear stress hypothesis. Meng et al. (2014) also proposed a low WSS hypothesis discussed in this section. In the paper on computational modelling of aneurysm growth, Selimovic et al. (2013) report that when elastin degradation was associated with high WSS this led to aneurysm formation, but of the fusiform type rather than the saccular type. Linking low WSS to elastin degradation resulted in formation of a saccular aneurysm. Selimovic et al. note that a possible mechanism for low-WSS initiation is the release of matrix-metalloproteinases (MMPs) by inflammatory cells, which degrade elastin.
- Flow instability hypothesis. In their study on computational modelling of aneurysms Selimovic et al. note that it may actually not be the magnitude of the WSS which is important, but the nature of the flow including flow oscillation and instability.

16.2.3.2 Growth of Saccular CAs

- High wall shear stress hypothesis. In an established aneurysm with impact of a jet on the dome (Fig. 16.2c), there will be a region of high WSS. This high WSS is detected by the endothelium, which in the early stages of aneurysm development is still intact, leading to release of MMPs and matrix degradation. There may be a local bleb formed at the region of impact. Remodelling of collagen stablises the aneurysm.
- Low wall shear stress hypothesis. In an established aneurysm where there is recirculating flow (Fig. 16.2b) the wall shear stress will be low. This low WSS is sensed by the endothelium, which in the early stages of aneurysm development, is still intact. This also leads to release of MMPS, but by an inflammatory route, which also leads to matrix degradation.

16.2.3.3 Rupture of Saccular CAs

A possible sequence of events concerning rupture is described here. Rupture occurs when the circumferential stress exceeds the local wall strength. Wall shear stress itself is too small a force to cause rupture. However the growth of the aneurysm is effected by WSS, causing changes to the wall which leave the aneurysm vulnerable to rupture. Following on from the above sub-section, where there is loss of matrix material, the aneurysm remodels in an attempt to achieve mechanical stability. This process must rely on an intact endothelium in order to drive remodelling. It is however noted above that aneurysms are commonly associated with loss of endothelium which must mean that at some point the remodelling apparatus is also

lost. With loss of endothelium driven remodelling the aneurysm is unable to mechanically stabilise itself and after this point the aneurysm is at risk of rupture.

16.2.4 In Vivo Imaging and Patient Specific Modelling

Traditional visualisation of CAs was undertaken using angiography which involved an arterial puncture. A number of non-invasive techniques have been used to diagnose the presence of CAs including CT angiography (CTA), rotational angiography (RA) and magnetic resonance angiography (MRA). All these techniques provide 3D data from which measurements may be made of aneurysm dimensions. In addition the 3D geometries may be used to derive indices describing shape and as the input to patient specific modelling. Ultrasound systems may also be used for visualisation of CAs. Further reading on the imaging of cerebral aneurysm is provided in Hoskins et al. (2011).

16.2.4.1 Measurements of Size

The measurements commonly made on a saccular aneurysm are illustrated in Fig. 16.3. The diameter of a saccular aneurysm is measured as the largest of the height (*H*), and the 2 orthogonal widths. As noted above the aneurysm is classified according to diameter (small <15 mm diameter, large 15–25 mm, giant 25–50 mm, super-giant >50 mm); and risk of rupture increase with diameter (Wermer et al. 2007).

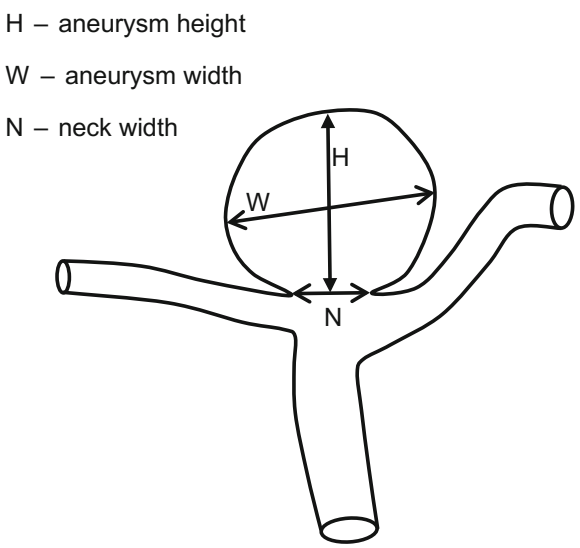

Fig. 16.3 Definition of dimensions of a saccular aneurysm measured from medical imaging data

The aspect ratio is the ratio of aneurysm height to neck width (Eq. 16.5).

$$\text{Aspect ratio} = \frac{\text{aneurysm height}}{\text{neck width}} \tag{16.5}$$

Aneurysms with a higher aspect ratio are at greater risk of rupture (Dhar et al. 2008; Ujiie et al. Ujiie et al. 1999; Weir et al. 2003; Nader-Sepahi et al. 2004), so this measurement may be used for clinical evaluation. The aspect ratio may also be used to help plan therapy; a ratio of >2 is considered as favourable for coil occlusion (Meyers et al. 2009). Measurement of aneurysm volume helps define the size of coil or balloon needed in therapeutic treatment. More complex shape descriptors involving the whole 3D geometry have been developed in research studies, whose details are outside the scope of this book (Millán et al. 2007).

16.2.4.2 Pulsatility

The aneurysm will change volume during the cardiac cycle as a result of the change in blood pressure. Dynamic CTA has been used to measure this change in volume (Hayakawa et al. 2005; Ishida et al. 2005; Krings et al. 2009). Ishida et al. (2005) noted pulsation in 9 of 28 saccular aneurysms and in 3 of 5 non-saccular aneurysms. Hayakawa et al. (2005) investigated 23 patients with ruptured aneurysms, of which 4 showed pulsation whose location corresponded to the site of rupture in all 4 cases. It was hypothesised in these studies that the pulsation occurred where the wall was thin, and that this was a site at risk of rupture.

16.2.4.3 Haemodynamics and Wall Stress

MRI may be used to measure blood velocities from which 3D data on haemodynamic flow patterns and wall shear stress may be calculated (Moftakhar et al. 2007). Haemodynamics may also be obtained as the output from patient specific modelling (see Chap. 11). Figure 16.4 shows examples of flow streamlines and wall shear stress in a saccular aneurysm. Patient specific modelling may also be used to estimate the distribution of circumferential wall stress (Fig. 16.5).

16.2.5 Treatment

This section presents a very brief description of the treatment of CAs. Further reading on diagnostic and treatment pathways are provided in Wardlaw and White (2000) and Mehrar et al. (2011). Most CAs that rupture are undiagnosed at the time of rupture and present as an emergency. Treatment of the ruptured aneurysm involves exclusion of the aneurysm from the circulation. The decision to treat the

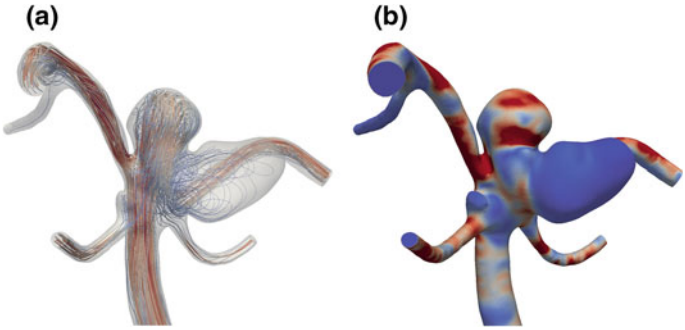

Fig. 16.4 Haemodynamics in a Basilar tip aneurysm with two lobes calculated from patient specific modelling. The basilar artery enters from the bottom of the image and is nearly vertical. **a** Flow streamlines; the velocity range is 0–2 ms^{-1}. **b** Wall shear stress; the range is 0–50 Pa. Images kindly provided by Dr. Arjan Geers (Edinburgh University). In both figures, red is 'high' and blue is 'low' ends of the range

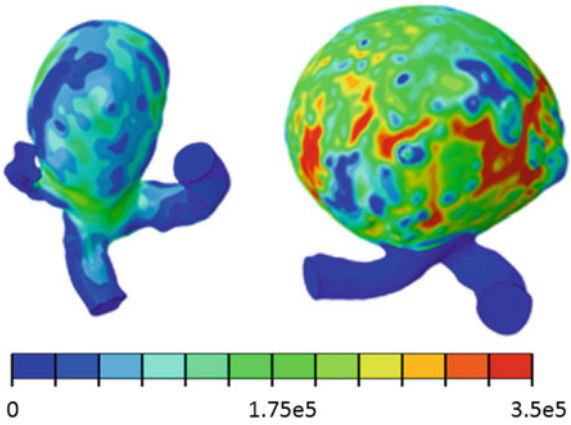

Fig. 16.5 von Mises stress (Pa) in cerebral aneurysms calculated from patient specific modelling. Image kindly provided by Dr. Noel Conlisk (Edinburgh University)

unruptured aneurysm is based on aneurysm diameter. Treatment is considered if the diameter is greater than 7 mm, however if there are other risk factors then treatment is considered if the diameter is greater than 3 mm diameter. Historically surgical clipping of the aneurysm was the preferred method for treatment of a cerebral aneurysm. This is highly invasive involving open surgery with placement of a clip across the aneurysm neck to separate the aneurysm from the main arterial flow channel. It is much more common to perform intervention by catheter based techniques under fluoroscopic guidance (White et al. 2015). The most common technique is the insertion of coils in the aneurysm which are thrombogenic, so that the aneurysm is sealed off by the presence of thrombus. Increasingly coiling is combined with the placement of a stent. The stent helps prevent ingress of the coil into the main arterial channel, hence allowing more aggressive coil placement, and provides a mesh on which an endothelium can grow. Other devices and methods

which are used in interventional treatment include balloon remodelling, flow diverters and intrasaccular flow disruptors.

16.3 Abdominal Aortic Aneurysms

16.3.1 Abdominal Aortic Aneurysm Disease

As the name implies, AAAs are localised increases in the diameter of the abdominal aorta (see Fig. 16.6), however they can often extend distally beyond the iliac bifurcation, or begin above the abdominal aorta. They are defined as a maximum aortic diameter ≥3.0 cm with the un-diseased diameter being around 2 cm. The incidence rates of AAAs range from 2 to 8 % for men over 65 years and the prevalence is 4 times lower in women. Over recent years, the incidence rates appear to be falling, with this being attributed to the change in smoking habits in developed countries (Lederle 2011).

Most AAAs are asymptomatic so that the first time the patient is aware of an aneurysm is after rupture. The most common symptom is sudden pain in the abdomen; other symptoms include low blood pressure, loss of consciousness and a pulsatile mass in the abdomen. Following rupture there is usually considerable internal bleeding and this is the main cause of death. If an unruptured AAA is detected, usually with medical imaging, the primary criterion determining surgical intervention is the size of the AAA, more specifically, the maximum diameter. If the maximum anterior-posterior diameter of the AAA exceeds 5.5 cm in men or 5.0 cm in women, and the patient is fit for surgery, repair is offered. Risk of rupture increases with maximum AAA diameter. The annual rupture risk increases from 0.5

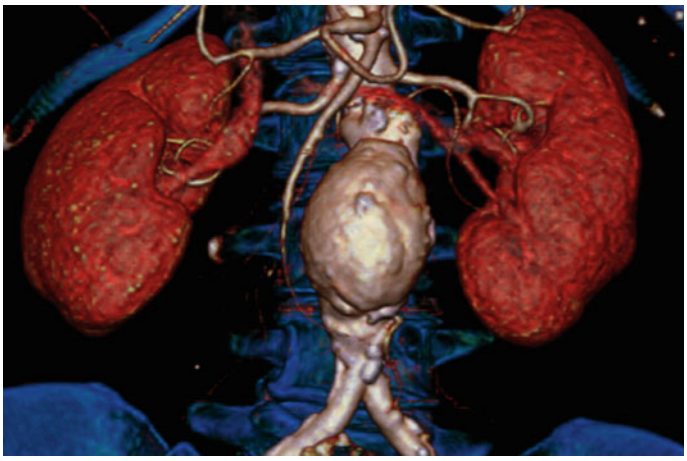

Fig. 16.6 CT reconstruction of an abdominal aortic aneurysm

to 5 % for diameter of 4.0–4.9 cm, 3–5 % for 5.0–5.9 cm, 10–20 % for 6.0–6.9 cm, and 20–40 % for 7.0–7.9 cm (Brewster et al. 2003).

A minority of AAA are symptomatic in that the patient develops a variety of symptoms associated with imminent rupture. These symptoms include abdominal pain, lower back pain and a pulsatile abdominal mass. Generally symptomatic patients are offered urgent repair of their AAA (De Martino et al. 2010).

16.3.2 Mechanics and Haemodynamics

The healthy aorta is often approximated as a cylinder; however, AAAs can develop into highly irregular shapes with regions of high curvature and highly tortuous centrelines. As such, the mechanics used to determine the stresses and strains cannot be approximated using the Law of Laplace (see Chap. 5.1.5). It is these stresses and strains that contribute to the growth, remodelling and eventual rupture of the AAA, hence the large research focus aimed at accurately predicting them (see Chap. 11.4.3). A material will fail when the local stress exceeds the local strength, and although there are many biological processes also at play, this general understanding also applies to AAA. Using patient specific modelling (PSM—discussed in detail in Chap. 11), it is possible to estimate the stress acting on the AAA wall in vivo (Fillinger et al. 2002, 2003; Truijers et al. 2007; Doyle et al. 2009; Gasser et al. 2010; Doyle et al. 2014). By coupling this data with knowledge of the AAA wall strength (Thubrikar et al. 2001; Raghavan et al. 2011, 2006), it is possible to determine the likelihood of rupture. However, predicting in vivo wall strength remains a significant challenge (vande Geest et al. 2006; Reeps et al. 2013).

Loss of elastin and increase in collagen content as the AAA grows leads to overall stiffening of the AAA vessel wall. The wall motion (difference in diameter between diastole and systole) is typically 10 % of the diameter in healthy arteries, so for a 20 mm diameter normal abdominal aorta the wall motion is around 2 mm. In a study performed on patients with AAA the average wall motion measured using an ultrasound system was only 1 mm (Wilson et al. 2003).

The majority ($\sim$75 %) of clinically-relevant AAAs have intraluminal thrombus (ILT) in the sac region. This ILT is a complex fibrin structure, with a continuous network of canaliculi, platelets, red blood cells and other haematopoietic cells, and its' role in AAA mechanics is still poorly understood. ILT starves the AAA wall of oxygen and thus weakens it (Vorp et al. 2001), yet appears to 'anchor' the wall and reduce wall deformation over the cardiac cycle. However, it allows the transmittance of the full pressure load to the wall (Schurink et al. 2000). The mechanical problem is further compounded by the fact that ILT develops in a patient-specific manner and can range from a relatively structured material to an unstructured one (see Fig. 16.7).

Information on the detailed mechanical properties of AAA tissues including thrombus arises from tensile testing performed on specimens of material gathered when surgery is performed. These properties are of interest in themselves for

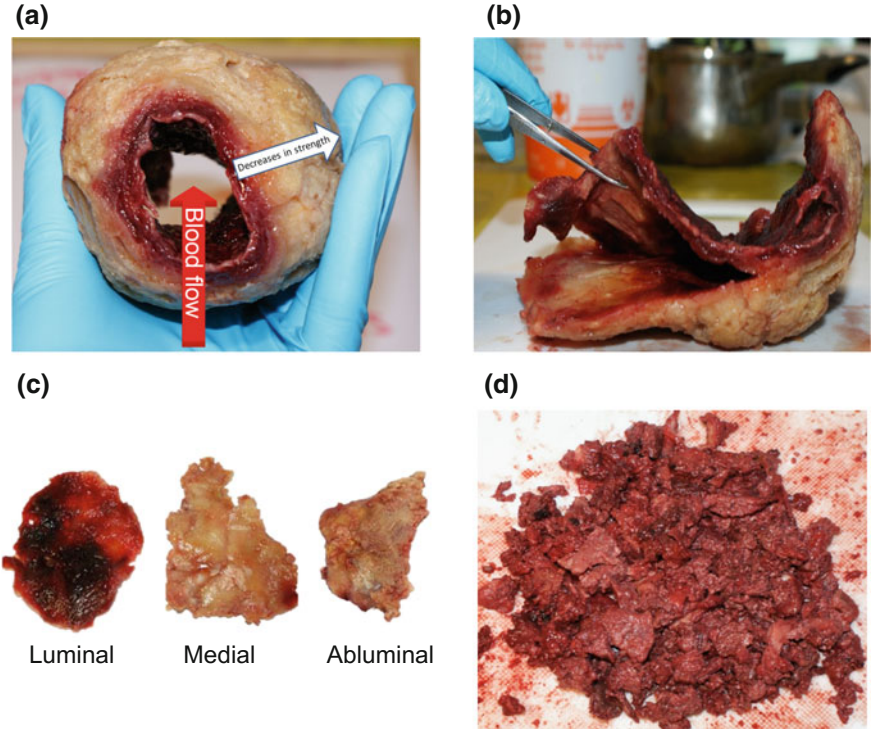

Fig. 16.7 The morphology of intraluminal thrombus (ILT). **a** Gross appearance of excised ILT, **b** separation of a structured ILT specimen into **c** the various layers (luminal, medial and abluminal), and **d** an unstructured ILT

understanding of the progression of AAA, and essential for PSM where assumed mechanical properties are imposed in a finite element analysis (FEA) framework. Material constants for a hyperelastic, homogeneous, incompressible, and isotropic constitutive model were provided by fitting experimental data; for the vessel wall (Raghavan and Vorp 2000) and for the thrombus (Wang et al. 2001). More sophisticated biaxial test methods are also possible, as discussed in Chap. 13. Further details of research studies on the mechanical properties of AAA thrombus and vessel wall are provided by Vorp (2007).

In conjunction with the structural mechanics at play, the haemodynamics in AAA are also crucial. As the aneurysm gradually expands, the geometry can become highly irregular, whereby the blood flow is complex. Flow into a tube where diameter increases causes an adverse pressure gradient leading to vortex formation at the edge of the tube. Curvature leads to changes in direction of flow including helical flow. In addition it is clear that there is already helical flow at the inlet to the AAA, which further enhances helical tendencies (Hardman et al. 2013); see Fig. 11.7a, d in Chap. 11. The nature of the flow contributes to the development of ILT and it has been shown that the residence time of platelets, red blood cells and

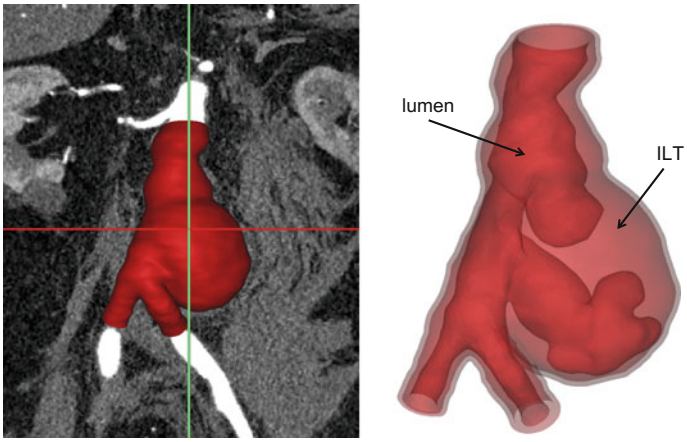

Fig. 16.8 (*Left*) 3D reconstructions of AAA from CT data and (*right*) the complicated lumen geometry as a result of ILT formation

other particles suspended in the blood, as well as the presence of vortical structures, calculated using PSM techniques, predicts the location of ILT build up (Biasetti et al. 2010, 2011; Basciano et al. 2011; Di Achille et al. 2014). In particular, the lumen of the AAA (that is, the blood channel) can form pockets surrounded by ILT (see Fig. 16.8). These pockets harbour stagnant, recirculating flow that contributes to further build-up of ILT and other biological processes.

16.3.3 Initiation, Growth and Rupture

As with CAs, the initiation, growth and rupture of AAA is a complex interplay of mechanical forces and biology. The exact cause of an aneurysm is still not known, however, it is widely accepted that the role of haemodynamics and wall shear stresses in the aorta, contribute to the initiation. In the healthy aorta, the innermost layer is the endothelium. As discussed in Chap. 5.4, haemodynamic forces in the aorta can upset this layer (as with all cardiovascular disease), especially in regions of abnormal flow. The continued exposure of the abdominal aorta to disturbed flow and the change in arterial microstructure with age, is thought to contribute to aneurysm initiation, and furthermore, growth.

As mentioned earlier, AAA is associated with a loss of elastin. Potential causes of elastin degradation are discussed by Lasheras (2007):

- Ageing. Over time repeated cycling of the elastin fibres during the cardiac cycle will lead to fibre fracture. Compensatory collagen deposition leads to stiffening of the aorta and a local increase in systolic pressure further exacerbating elastin fibre degradation.

- Wall shear. The normal abdominal aorta will increase in diameter over time as a response to stiffening of the aorta. This may lead to increased tortuosity, which will give rise to regions of abnormal wall shear; for example low wall shear has been associated with elastin loss.

Studies which describe models of AAA initiation and growth are described by Sheidaei et al. (2011), and this growth and remodelling (G&R) of AAA is a highly active research area (Watton et al. 2004; Humphrey 2008; Sheidaei et al. 2011; Zeinali-Davarani et al. 2011; Humphrey and Holzapfel 2012; Grytsan et al. 2015). The growth of AAA is largely due to the change in microstructure. AAAs are characterised by a thinning medial layer with a reduction in elastin and an increased turnover of collagen. This knowledge has led to computational models of G&R that account for microstructural changes and result in AAA expansion due to the haemodynamic load (Fig. 16.9).

The likely chain of events leading to rupture is shown in Fig. 16.10. Although fundamentally, the AAA will rupture when stress exceeds strength, the chain of events leading to wall weakening (and thus, increases in stress) is not trivial. For a detailed review of the biological factors influencing AAA rupture, see (Choke et al. 2005).

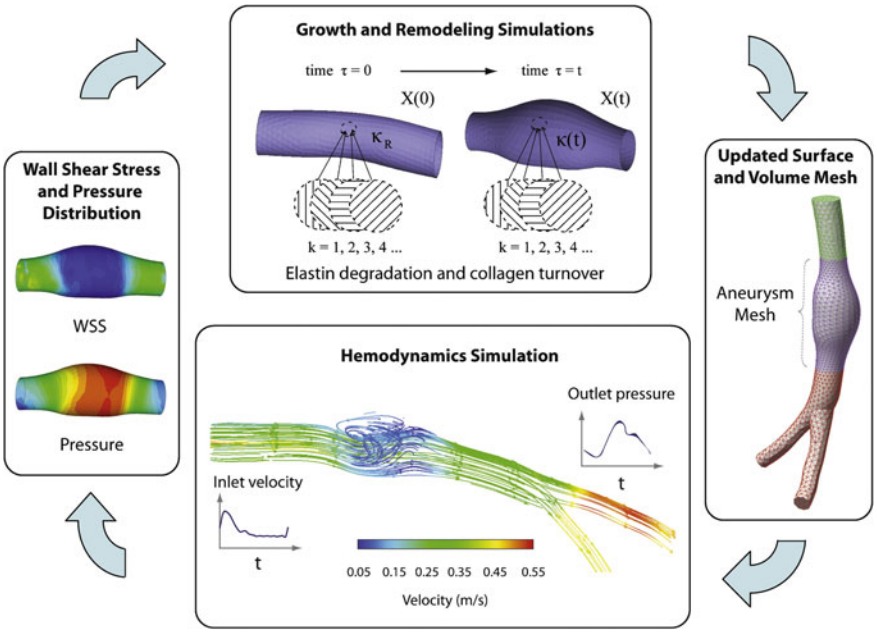

Fig. 16.9 A computational growth and remodelling (G&R) framework. Iterative loop and information transfer in the coupling between the haemodynamics and G&R simulations. Reprinted from Medical Engineering & Physics, Vol. 33(1), Sheidaei A, Hunley SC, Zeinali-Davarani S, Raguin LG, Baek S; Simulation of abdominal aortic aneurysm growth with updating hemodynamic loads using a realistic geometry. pp. 80–88, Copyright (2011), with permission from the Institute of Physics and Engineering in Medicine and Biology

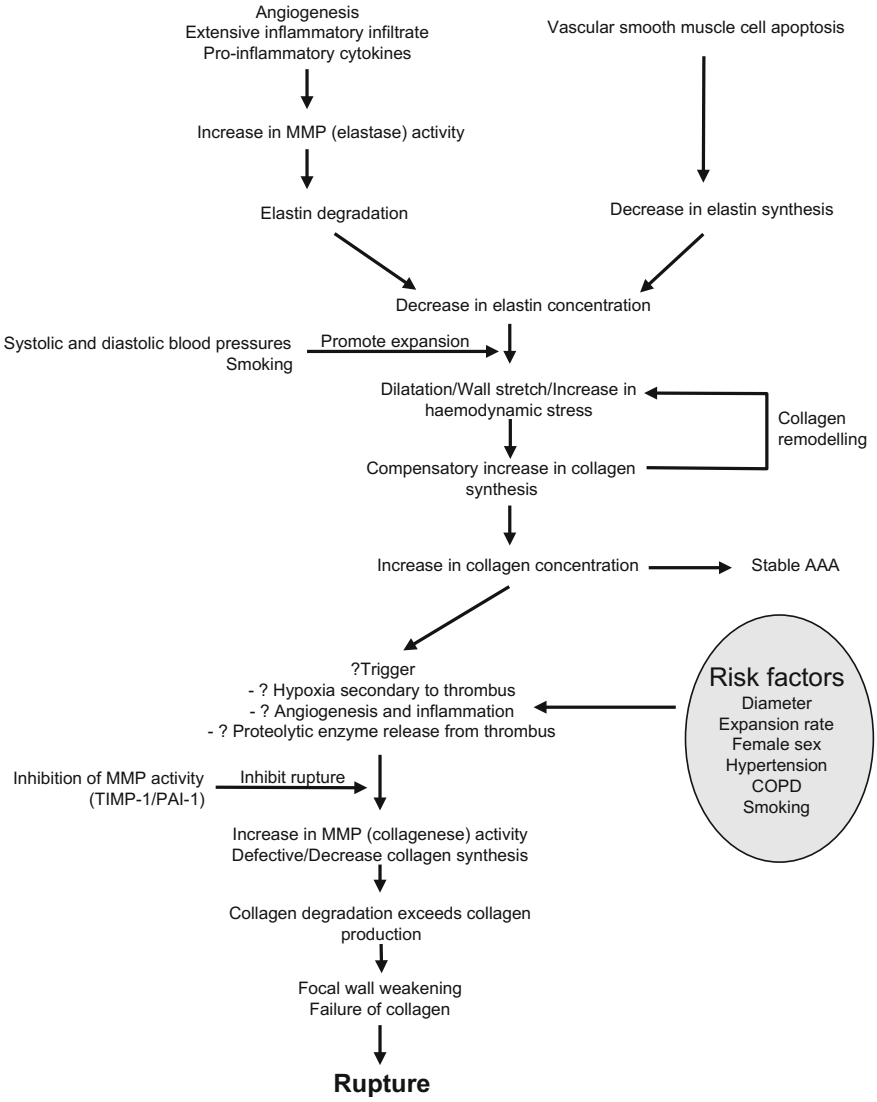

Fig. 16.10 Chain of biological events leading to AAA rupture. Reprinted from European Journal of Vascular and Endovascular Surgery, Vol. 30(3), Choke E, Cockerill G, Wilson WR, Sayed S, Dawson J, Loftus I, Thompson MM. A review of biological factors implicated in abdominal aortic aneurysm rupture. pp. 227–244, Copyright (2005), with permission from Elsevier

16.3.4 In Vivo Imaging and Patient Specific Modelling

In clinical practice, ultrasound imaging is the most common method of evaluating the size of an AAA. The maximum diameter is measured using B-mode imaging

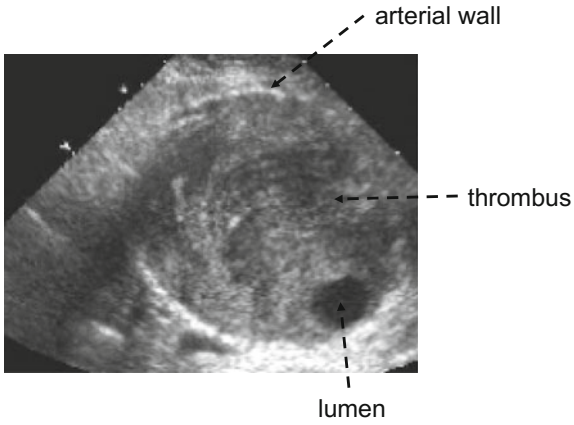

Fig. 16.11 In vivo ultrasound image of AAA

(Fig. 16.11). CT scanning is performed to evaluate if the AAA has ruptured, or to assist in planning of surgical intervention. For use in patient specific modelling, 3D geometry is provided from CT or MRI, as discussed in Chap. 11.

16.3.4.1 AAA Symmetry

As described earlier, the decision to undertake elective surgery is mostly based on maximum diameter. In the research literature, shape descriptors have been formulated based on an analysis of the 3D data from CT. One such descriptor is the

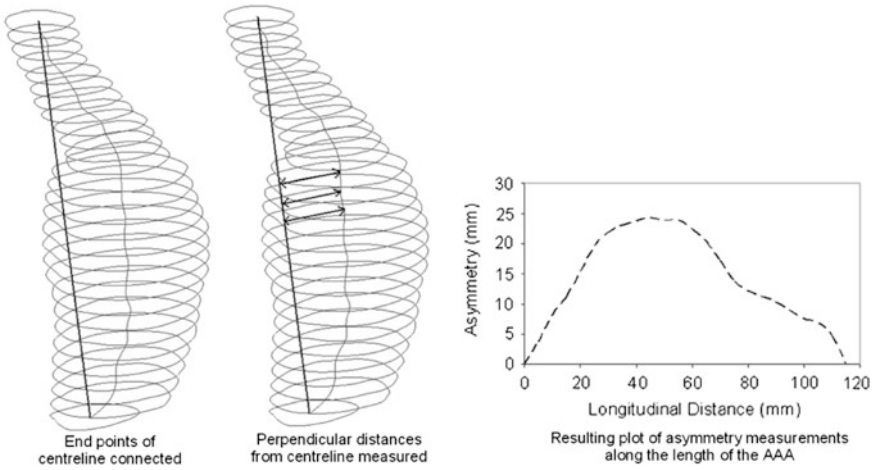

Fig. 16.12 The asymmetry method for AAA. Reprinted from Journal of Vascular Surgery, Vol. 49 (2), Doyle BJ, Callanan A, Burke PE, Grace PA, Walsh MT, Vorp DA, McGloughlin TM. Vessel asymmetry as an additional diagnostic tool in the assessment of abdominal aortic aneurysms. pp. 443–454, Copyright (2009), with permission from The Society for Vascular Surgery

asymmetry index as illustrated in Fig. 16.12 (Doyle et al. 2009). The analysis starts with identification of the centre of the vessel for each slice of the CT scan. The inlet and the outlet centre points are connected with a straight line. The deviation from the centreline is measured and plotted. The asymmetry index is defined as the maximum deviation. It has been argued that the asymmetry index is a surrogate for peak wall stress; in that AAA which are more asymmetric have higher peak wall stress.

In general shape indices rely only on information from the CT scan so could be implemented easily in clinical practice whereas biomechanics-based rupture risk requires a patient specific modelling workflow.

16.3.4.2 Wall Motion and Pressure Strain Elastic Modulus

The radial motion of the vessel wall during the cardiac cycle may be measured using ultrasound. A number of different techniques have been used (Hoeks et al. 1999) of which correlation of the RF data from consecutive image lines is probably the most widely used. Using these techniques displacements in the range 1–10 micron can easily be measured. This is sufficient to provide good accuracy for typical AAA diameter changes of 0.5–3 mm. From the measured wall motion, a measure of wall stiffness may be measured called the 'pressure strain elastic modulus' E_p, first formulated by Peterson et al. (1960).

$$E_p = \frac{P_s - P_d}{(d_s - d_d)/d_d} \tag{16.6}$$

where P_s and P_d are systolic and diastolic pressure, d_s and d_d are systolic and diastolic diameter.

Pressure values within the AAA are difficult to obtain and in practice, pressure values taken with an arm cuff are used. Stiffness of AAA using this methodology was measured in AAA by Wilson et al. (2003) where it was shown that there was no difference between in stiffness in patients who ruptured, compared to patients who did not.

In this approach the assumed physical model is that the artery consists of an elastic cylinder of uniform wall thickness and uniform elasticity. In reality, an AAA is a complex 3D structure with variations in wall thickness and mechanical properties, suggesting that more complex methods able to account for these 3D variations are needed.

16.3.4.3 Haemodynamics and Wall Stress

MRI techniques may be used to estimate flow-field data from which wall shear stress may, in principle, be estimated. In practice, it is more common to use a patient specific modelling approach involving computational fluid dynamics for the

estimation of wall shear stress (Fig. 16.13). Outward expansion of the lumen is associated with regions of low wall shear stress and high residence time for blood particles, such as platelets.

Patient specific modelling, using FEA, may also be used for the estimation of stress within the wall; see Chap. 11. Typically the von-Mises stress is calculated which is a composite of the various stresses estimated using FEA. Surprisingly in this area there are few clinical studies. Figure 16.14 shows peak wall stress in different groups of AAA patients from Fillinger et al. (2003). In the lowest risk group patients have AAA with diameter <5.5 cm and attend a surveillance programme. The group with the next highest risk have diameters greater than 5.5 cm and are being considered for elective surgery. The highest risk group are those who went on to rupture or presented with symptoms of imminent rupture such as severe back pain. Diameter increases with risk, as would be expected. Also peak wall stress increases with risk. The ROC plot shows that overall categorisation is performed better by peak wall stress.

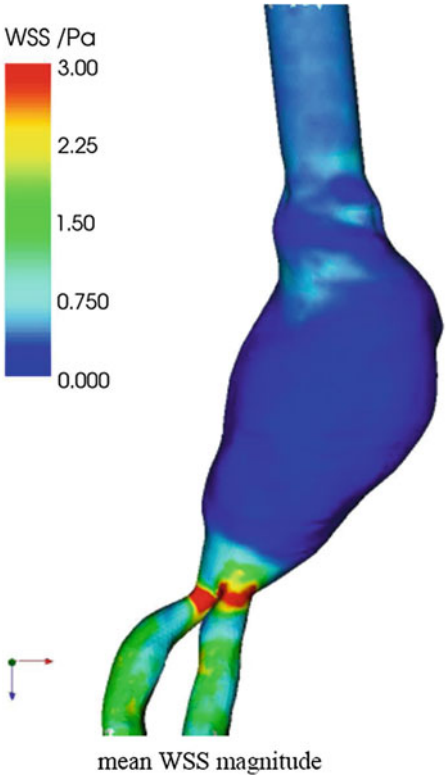

Fig. 16.13 Distribution of wall shear stress (WSS) in AAA

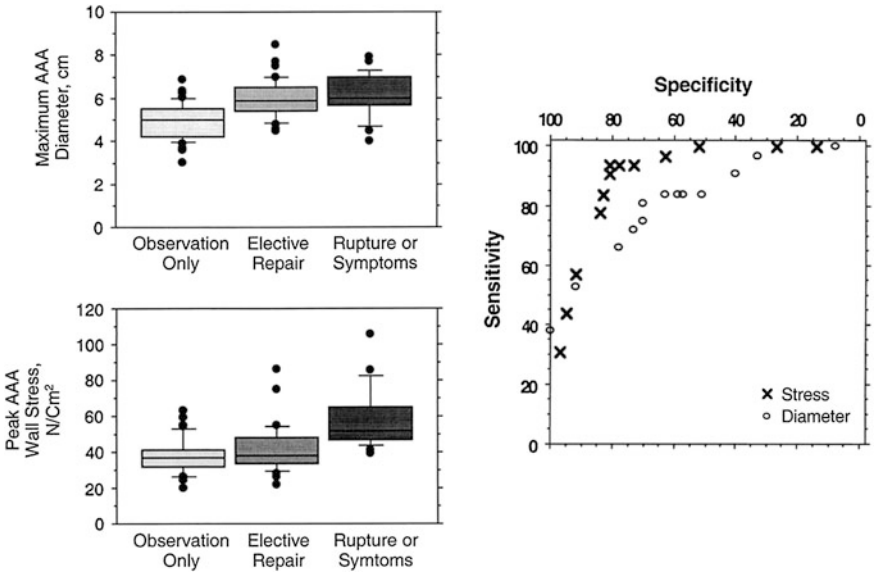

Fig. 16.14 *Top left* box plot for AAA diameter demonstrates that 90 % of AAAs under observation have diameter larger than the lowest recorded diameter for an AAA that subsequently ruptured or became symptomatic, which was 4.4 cm in maximum diameter. *Bottom left* box plot for peak AAA wall stress demonstrates that 75 % of AAAs under observation have stress lower than the lowest recorded stress for an AAA that subsequently ruptured or became symptomatic. *Right* receiver operating characteristic curves shows superior sensitivity and specificity of peak wall stress in comparison with diameter throughout the clinically important range. Reprinted from Journal of Vascular Surgery, Vol. 37(4), Fillinger MF, Marra SP, Raghavan ML, Kennedy FE. Prediction of rupture risk in abdominal aortic aneurysm during observation: wall stress versus diameter. pp. 724–732, Copyright (2003), with permission from The Society for Vascular Surgery and The American Association for Vascular Surgery

16.3.5 Diagnosis and Treatment

In the absence of a screening programme, most AAA are diagnosed following rupture or through chance findings during imaging investigations for other medical problems. A UK-wide AAA screening programme has been in operation since 2013 with men aged over 65 years are offered an ultrasound scan to measure the diameter of their abdominal aorta. If an AAA is found (diameter >3 cm) the patient is put on a surveillance programme with measurements every 6 months. Generally AAA grow in size. When the diameter exceeds 5.5 cm the patient is considered for elective surgery. The measure of risk of rupture of an AAA is based largely on the maximum diameter. This diameter criterion stems from early autopsy data (Darling et al. 1977) that noted cases over 5.0 cm ($\sim$40 %) are more likely to rupture. However, the same report also showed many larger AAAs were still intact after death and many smaller ones did not burst ($\sim$13 %). The criteria of 5.5 cm was set

following clinical trials performed in the 1990s (UKSAT 1998). In addition the growth rate (i.e. change in diameter over time) is also recorded and a growth rate of greater than ≥1.0 cm/year is considered an indicator of imminent rupture.

Traditional repair of an AAA involved open surgery and replacement of the AAA with a synthetic graft, which is connected to the aorta with stitches. The operation involves removal of the thrombus, if present. The original AAA wall is trimmed to allow the wall to be wrapped around the graft. This traditional open repair is increasingly being replaced by a less invasive method involving endovascular stenting (endovascular aneurysm repair or EVAR). Access is gained through the femoral artery and an expanding stent graft is located within the AAA under fluoroscopic guidance.

More details of AAA diagnosis, imaging and treatment are provided in Hoskins et al. (2011).

References

Basciano C, Kleinstreuer C, Hyun S, Finol EA. A relation between near-wall particle-hemodynamics and onset of thrombus formation in abdominal aortic aneurysms. Ann Biomed Eng. 2011;39:2010–26.

Biasetti J, Gasser TC, Auer M, Hedin U, Labruto F. Hemodynamics of the normal aorta compared to fusiform and saccular abdominal aortic aneurysms with emphasis on a potential thrombus formation mechanism. Ann Biomed Eng. 2010;38:380–90.

Biasetti J, Hussain F, Gasser TC. Blood flow and coherent vortices in the normal and aneurysmatic aortas: a fluid dynamical approach to intra-luminal thrombus formation. J R Soc Interface. 2011;8:1449–61.

Brewster DC, Cronenwett JL, Hallett JW Jr, et al. Guidelines for the treatment of abdominal aortic aneurysms. Report of a subcommittee of the Joint Council of the American Association for Vascular Surgery and Society for Vascular Surgery. J Vasc Surg. 2003;37:1106–17.

Brisman JL, Song JK, Newell DW. Cerebral aneurysms. New Eng J Med. 2006;355:928–39.

Choke E, Cockerill G, Wilson WR, Sayed S, Dawson J, Loftus I, Thompson MM. A review of biological factors implicated in abdominal aortic aneurysm rupture. Eur J Vasc Endovasc Surg. 2005;30:227–44.

Darling RC, Messina CR, Brewster DC, Ottinger LW. Autopsy study of unoperated abdominal aortic aneurysms. The case for early resection. Circulation. 1977;56(3 Suppl):II 161–164.

De Martino RR, Nolan BW, Goodney PP, Chang CK, et al. Outcomes of symptomatic abdominal aortic aneurysm repair. J Vasc Surg. 2010;52:5–12.

Dhar S, Tremmel M, Mocco J, Kim M, Yamamoto J, Siddiqui AH, Hopkins LN, Meng H. Morphology parameters for intracranial aneurysm rupture risk assessment. Neurosurgery. 2008;63:185–96.

Di Achille P, Tellides G, Figueroa CA, Humphrey JD. A haemodynamic predictor of intraluminal thrombus formation in abdominal aortic aneurysms. Proc Royal Soc Lond A Math Phys Eng Sci. 2014;470:0163.

Doyle BJ, Callanan A, Burke PE, Grace PA, Walsh MT, Vorp DA, McGloughlin TM. Vessel asymmetry as an additional diagnostic tool in the assessment of abdominal aortic aneurysms. J Vasc Surg. 2009;49:443–54.

Doyle BJ, McGloughlin TM, Miller K, Powell JT, Norman PE. Regions of high wall stress can predict the future location of rupture of abdominal aortic aneurysm. Cardiovasc Intervent Radiol. 2014;37:815–8.

Fillinger MF, Raghavan ML, Marra SP, Cronenwett JL, Kennedy FE. In vivo analysis of mechanical wall stress and abdominal aortic aneurysm rupture risk. J Vasc Surg. 2002;36:589–97.

Fillinger MF, Marra SP, Raghavan ML, Kennedy FE. Prediction of rupture risk in abdominal aortic aneurysm during observation: wall stress versus diameter. J Vasc Surg. 2003;37:724–32.

Frösen J, Piippo A, Paetau A, Kangasniemi M, Niemelä M, Hernesniemi J, Jääskeläinen J. Remodeling of saccular cerebral artery aneurysm wall is associated with rupture: histological analysis of 24 unruptured and 42 ruptured cases. Stroke. 2004;35:2287–93.

Frösen J, Tulamo R, Paetau A, Laaksamo E, Korja M, Laakso A, Niemelä M, Hernesniemi J. Saccular intracranial aneurysm: pathology and mechanisms. Acta Neuropathol. 2012;123:773–86.

Gasser TC, Auer M, Labruto F, Swedenborg J, Roy J. Biomechanical rupture risk assessment of abdominal aortic aneurysms: model complexity versus predictability of finite element simulations. Eur J Vasc Endovasc Surg. 2010;40:176–85.

Grytsan A, Watton PN, Holzapfel GA. A thick-walled fluid-solid-growth model of abdominal aortic aneurysm evolution: application to a patient-specific geometry. J Biomech Eng. 2015;137. doi:10.1115/1.4029279.

Hardman D, Semple SIK, Richards JMJ, Hoskins PR. Comparison of patient specific inlet boundary conditions in the numerical modelling of blood flow in abdominal aortic aneurysm disease. Int J Num Meth Biomed Eng. 2013;29:165–78.

Hayakawa M, Katada K, Anno H, Imizu S, Hayashi J, Irie K, Negoro M, Kato Y, Kanno T, Sano H. CT angiography with electrocardiographically gated reconstruction for visualizing pulsation of intracranial aneurysms: identification of aneurysmal protuberance presumably associated with wall thinning. Am J Neuroradiol. 2005;26:1366–9.

Hoeks APG, Brands PJ, Willigers JM, Reneman RS. Noninvasive measurement of mechanical properties of arteries in health and disease. J Eng Med. 1999;213:195–202.

Hoskins PR, Semple S, White P, Richards J. Imaging of aneurysms. In: McGloughlin T, editor. Biomechanics and mechanobiology of aneurysms. Berlin: Springer; 2011. p. 35–65.

Humphrey JD. Vascular adaptation and mechanical homeostasis at tissue, cellular, and sub-cellular levels. Cell Biochem Biophys. 2008;50:53–78.

Humphrey JD, Taylor CA. Intracranial and abdominal aortic aneurysms: similarities, differences, and need for a new class of computational models. Annu Rev Biomed Eng. 2008;10:221–46.

Humphrey JD, Holzapfel GA. Mechanics, mechanobiology, and modeling of human abdominal aorta and aneurysms. J Biomech. 2012;45:805–14.

Ishida F, Ogawa H, Simizu T, Kojima T, Taki W. Visualizing the dynamics of cerebral aneurysms with four-dimensional computed tomographic angiography. Neurosurgery. 2005;57:460–470.

Juvela S. Treatment options of unruptured intracranial aneurysms. Stroke. 2004;35:372–4.

Krings T, Willems P, Barfett J, Ellis M, Hinojosa N, Blobel J, Geibprasert S. Pulsatility of an intracavernous aneurysm demonstrated by dynamic 320-detector row CTA at high temporal resolution. Cen Eur Neurosurg. 2009;70:214–8.

Lasheras JC. The biomechanics of arterial aneurysms. Ann Rev Fluid Mech. 2007;39:293–319.

Lederle FA. The rise and fall of abdominal aortic aneurysm. Circulation. 2011;124:1097–9.

McGloughlin TM, Doyle BJ. New approaches to abdominal aortic aneurysm rupture risk assessment: engineering insights with clinical gain. Arterioscler Thromb Vasc Biol. 2010;30:1687–94.

Mehra M, Spilberg G, Gounis MJ, Wakhloo AK. Intracranial aneurysms: clinical assessment and treatment options. In: T McGloughlin, editor. Biomechanics and mechanobiology of aneurysms. Springer: Berlin; 2011. pp. 331–372.

Meng H, Tutino VM, Xiang J, Siddiqui A. High WSS or low WSS? Complex interactions of hemodynamics with intracranial aneurysm initiation, growth, and rupture: toward a unifying hypothesis. Am J Neuroradiol. 2014;35:1254–62.

Meyers P, Schumacher HC, Higashida RT, Derdeyn C, Nesbit GM, Sacks D, Wechsler L, Bederson J, Lavine S, Rasmussen P. Reporting standards for endovascular repair of saccular intracranial cerebral aneurysms. Stroke. 2009;40:e366–79.

Millán RD, Dempere-Marco L, Pozo JM, Cebral JR, Frangi AF. Morphological characterization of intracranial aneurysms using 3-D moment invariants. IEEE Trans Med Imag. 2007;26:1270–82.

Moftakhar R, Aagaard-Kienitz B, Johnson K, et al. Noninvasive measurement of intra-aneurysmal pressure and flow pattern using phase contrast with vastly undersampled isotropic projection imaging. Am J Neuroradiol. 2007;28:1710–4.

Nader-Sepahi A, Casimiro M, Sen J, et al. Is aspect ratio a reliable predictor of intracranial aneurysm rupture? Neurosurgery. 2004;54:1343–8.

Penn DL, Komotar RJ, Connolly ES. Hemodynamic mechanisms underlying cerebral aneurysm pathogenesis. J Clin Neurosci. 2011;18:1435–8.

Peterson LH, Jensen RE, Parnell R. Mechanical properties of arteries in vivo. Circ Res. 1960;8:622–639.

Raghavan ML, Vorp DA. Toward a biomechanical tool to evaluate rupture potential of abdominal aortic aneurysm: identification of a finite strain constitutive model and evaluation of its applicability. J Biomech. 2000;33:475–82.

Raghavan ML, Kratzberg J, de Tolosa EMC, Hanaoka MM, Walker P, da Silva ES. Regional distribution of wall thickness and failure properties of human abdominal aortic aneurysm. J Biomech. 2006;39:3010–6.

Raghavan ML, Hanaoka MM, Kratzberg JA, de Higuchi ML, da Silva ES. Biomechanical failure properties and microstructural content of ruptured and unruptured abdominal aortic aneurysms. J Biomech. 2011;44:2501–7.

Reeps C, Maier A, Pelisek J, Härtl F, Grabher-Meier V, Wall WA, Essler M, Eckstein HH, Gee MW. Measuring and modeling patient-specific distributions of material properties in abdominal aortic aneurysm wall. Biomech Model Mechanobiol. 2013;12:717–33.

Schurink GW, van Baalen JM, Visser MJ, van Bockel JH. Thrombus within an aortic aneurysm does not reduce pressure on the aneurysmal wall. J Vasc Surg. 2000;31:501–6.

Selimovic A, Ventikos Y, Watton PN. Modelling the evolution of cerebral aneurysms: Biomechanics, mechanobiology and multiscale modelling. Procedia IUTAM. 2013;10:396–409.

Sforza DM, Putman CM, Cebral JR. Hemodynamics of cerebral aneurysms. Ann Rev Fluid Mech. 2009;41:91–107.

Sheidaei A, Hunley SC, Zeinali-Davarani S, Raguin LG, Baek S. Simulation of abdominal aortic aneurysm growth with updating hemodynamic loads using a realistic geometry. Med Eng Phys. 2011;33:80–8.

Thubrikar MJ, Labrosse M, Robicsek F, Al-Soudi J, Fowler B. Mechanical properties of abdominal aortic aneurysm wall. J Med Eng Technol. 2001;25:133–42.

Truijers M, Pol JA, Schultzekool LJ, van Sterkenburg SM, Fillinger MF, Blankensteijn JD. Wall stress analysis in small asymptomatic, symptomatic and ruptured abdominal aortic aneurysms. Eur J Vasc Endovasc Surg. 2007;33:401–7.

Ujiie H, Tachibana H, Hiramatsu O. Effects of size and shape (aspect ratio) on the hemodynamics of saccular aneurysms: a possible index for surgical treatment of intracranial aneurysms. Neurosurgery. 1999;45:119–30.

vande Geest JP. Wang DHJ, Wisniewski SR, Makaroun MS, Vorp DA. Towards a noninvasive method for determination of patient-specific wall strength distribution in abdominal aortic aneurysms. Ann Biomed Eng. 2006;34:1098–2006.

Vorp DA. Biomechanics of abdominal aortic aneurysm. J Biomech. 2007;40:1887–902.

Vorp DA, Lee PC, Wang DH, Makaroun MS, Nemoto EM, Ogawa S, Webster MW. Association of intraluminal thrombus in abdominal aortic aneurysm with local hypoxia and wall weakening. J Vasc Surg. 2001;34:291–9.

Wang DHJ, Makaroun MS, Webster MW, Vorp DA. Mechanical properties and microstructure of intraluminal thrombus from abdominal aortic aneurysm. J Biomech Eng. 2001;123:536–9.

Wardlaw JM, White PM. The detection and management of unruptured intracranial aneurysms. Brain. 2000;123:205–21.

Watton PN, Hill NA, Heil M. A mathematical model for the growth of the abdominal aortic aneurysm. Biomech Model Mechanobiol. 2004;3:98–113.
Weir B, Amidei C, Kongable G, et al. The aspect ratio (dome/ neck) of ruptured and unruptured aneurysms. J Neurosurg. 2003;99:447–51.
Wermer MJ, van der Schaaf IC, Algra A, Rinkel GJ. Risk of rupture of unruptured intracranial aneurysms in relation to patient and aneurysm characteristics: an updated meta-analysis. Stroke. 2007;38:1404–10.
White P, duPlessisb J, Jayakrishnanc V, Mitrac D. An overview of the endovascular treatment of intracranial aneurysms. In: Lanzer P, editor. Pan vascular medicine. Berlin: Springer; 2015. p. 2497–535.
Wilson KA, Lee AJ, Lee AJ, Hoskins PR, Fowkes FGR, Ruckley CV, Bradbury AW. The relationship between aortic wall distensibility and rupture of infrarenal abdominal aortic aneurysms. J Vasc Surg. 2003;37:112–7.
Wong GK, Poon WS. Current status of computational fluid dynamics for cerebral aneurysms: the clinician's perspective. J Clin Neurosci. 2011;18:1285–8.
Zeinali-Davarani S, Sheidaei A. Baek S.A finite element model of stress-mediated vascular adaptation: application to abdominal aortic aneurysms. Comput Methods Biomech Biomed Eng. 2011;14:803–17.